# ADVANCED FLUX-GATE MAGNETOMETERS WITH LOW DRIFT

*Rikhard Berkman, Bogdan Bondaruk, Valery Korepanov*
Lviv Centre of Space Research Institute of National Academy of Sciences
and National Space Agency, Lviv, Ukraine

*Abstract:* Among various types of magnetometers the flux-gate ones seem to be the most convenient in order to get high class results by relatively low cost, both for observatory and land observations. Theoretical and technological approaches to the design of low-noise flux-gate magnetometers (FGM) are presented. Main of their peculiarity is so-called ferroresonance excitation mode, when the excitation winding of the mumetal core and its shunting capacitor form a non-linear oscillator with low active losses. As a result of theoretical and experimental study two main problems were revealed and eliminated - rather narrow area of stable parameters of excitation circuit and low stability of output signal phase. Some other new solutions were proposed in order to enlarge the dynamic band of the magnetometer: improved version of the feedback circuit and new design of the phase detector with the intermediate voltage-to-current transformer. New versions of one-component sensor for absolute measurements and corresponding electronics are discussed.

*Keywords:* flux-gate, magnetometer, thermal drift, geomagnetic.

The modern state of geomagnetic investigations needs very high accuracy of the obtained data. Among various types of magnetometers the flux-gate ones seem to be the most convenient in order to get high class results by relatively low cost. They are still the most widespread both for observatory and land observations of the Earth's magnetic field components. The recent developments in the technology of the flux-gate sensors (FS) design and manufacturing allowed to reach their noise level about a few pT. Also new more and more complicated requirements must be accomplished, especially as to the temperature and long-term stability. Some new theoretical and technological approaches to the design of the high class FGM with comparably low price are presented below.

One of the peculiarities of the developed magnetometers is so called ferroresonance excitation mode (FEM), when the excitation winding $W_e$ of flux-gate core and its shunting capacitance $C_k$ form a non-linear oscillator with low active losses.

Fig.1 presents the realization of FEM and fig.2 - diagrams of current and voltages in the circuit.

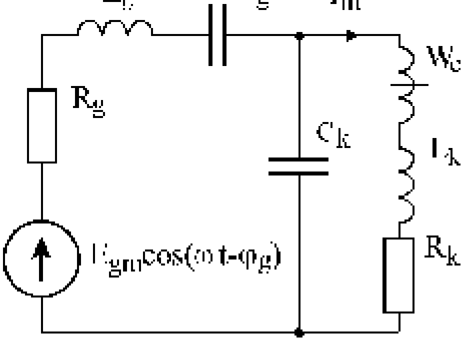


Fig.1. FEM schematic diagram.

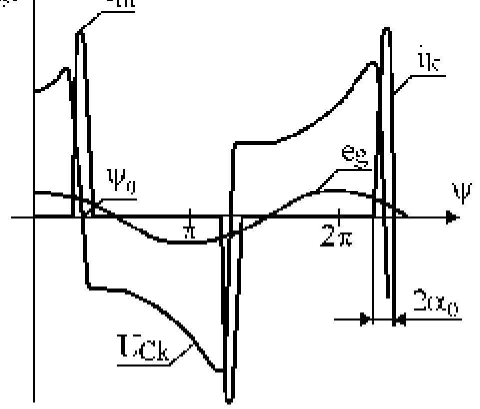


Fig.2. Voltage and current curves of FEM.

The series $L_gC_gC_k$ -circuit is tuned near the frequency ω of excitation source $E_g$. The main idea of FEM consists in the use of storing capacitance $C_k$ charge which is formed in the end of the demagnetization interval for the generation of discharge pulse of great amplitude at the saturation interval. Because of relatively short time of the saturation interval the energy input is sharply decreased, especially when discharge circuit has high Q- factor.

It should be noted that the coupling of the capacitance in parallel with the FS excitation windings was already used by some investigators (M.Acuna, B.Narod et al) with simple and physically clear aim to compensate the reactive power component in the excitation generator circuit. This aim was efficiently reached but only for FS excitation in circuits with relatively high losses, i.e., with low Q- factor of LC - circuits. The attempts to lower the power losses in the excitation circuit caused an instability with qualitatively different excitation modes in dependence from the initial conditions and from the way to approach the mode. It explains the fact that in known practically realized versions only moderate power saving was obtained in the modes of relatively low level FS cores saturation.

So, apparently similar excitation circuit realizations are drastically different as to the specifics of physical process. Especially it is so from the point of view of the analysis complexity. Only deep and thoroughful analysis of FEM based on non-linear circuits theory (and not on their linear approach) allowed to reveal in full volume both potential FEM advantages and inherent difficulties.

Using FEM, it is possible to have in the excitation winding current pulses $I_m$ (fig.2) achieving amperes, when mean consumed current is only tens of milliamperes and active losses in the winding are less than 0,05 watt. Such high amplitude of excitation field (2000 A/m and more) allows to eliminate hysteresis zero drift and its short duration lowers heat dissipation in the sensor volume. Additional advantages of FEM are the sensitivity stability and low noise level: typical values are 20 pT rms, lowest ones can be about 3 ÷ 5 pT.

In order to compare the known excitation modes their main parameters are assembled in the table 1.

Table 1. Comparison of main parameters of different excitation modes.

| Excitation mode / Parameter | Current sinu-soidal | Current tri-angular | Current trape-zium | Current step-wise rectan-gular | Voltage sinusoidal | Voltage rectan-gular | FEM |
|---|---|---|---|---|---|---|---|
| Sensitivity threshold * | + | 0 | 0 | 0 | + + | + | + + |
| Even harmonic error * | + | 0 | 0 | 0 | + + | + | + + |
| Generator voltage changes error * | + | + | + | + + | 0 | 0 | + + |
| Zero offset by overload * | 0 | 0 | 0 | + | + | + | + + |
| Sensitivity stability ** | 0 | 0 | 0 | + + | + | + | + + |
| Rapidity ** | + | + | 0 | 0 | + + | + + | + + |
| Self-heating of sensor ** | 0 | 0 | 0 | 0 | + | + | + + |
| Realization simplicity ** | + + | + | 0 | 0 | + + | + + | + |
| Analysis and calculation simplicity ** | + + | + + | + + | + + | 0 | + | 0 |

In this table for convenience: for * : ++ low; + medium; 0 high.
for **: 0 low; + medium; ++ high.

Also two problems arise when FEM is used: 1) stable ferroresonance oscillations are possible only in rather narrow area of parameters of the FS and excitation source Eg; 2) the phase of the FS output signal is much less stable as at another known modes. Both these disadvantages were eliminated as follows.

The analysis executed allowed to find the equations for calculation the region of stable oscillations in non-linear circuit:

$$\varepsilon_u = \left[ \frac{\left[\varepsilon_i bd + mb^2 \nu_c / (1+m)\right]^2 + \left\{\varepsilon_i\left[1 - b^2(1+m)\right] - mb^2 \nu_s / (1+m)\right\}^2}{(bd)^2 + \left(b^2 - 1\right)^2} \right]^{1/2} \quad (1)$$

where $\varepsilon_u$ - the excitation degree of the circuit by voltage; $\varepsilon_i$ - the same by current; b - relative deviation of resonance frequency $\omega_0$ of $L_gC_gC_k$ circuit from $\omega$; d - attenuation of circuit $L_gC_gR_gC_k$ ; $m = C_g / C_k$ ; $\nu_c$ and $\nu_s$ – the ratio between cosine and sine components of the first harmonic of voltage across the capacitor $C_k$ and $U_{mcr}$ - sinusoidal voltage amplitude across the same $C_k$, by which the induction in the core riches the ± Bs values.

Maximum and minimum values of $\varepsilon_u$, which determine the stability region boundaries of FEM, may be calculated (for small hysteresis losses), inserting in equation (1) the corresponding boundary values of excitation degree of the circuit by current - $\varepsilon_{i\,min}$ and $\varepsilon_{i\,max}$ :

$$\varepsilon_{i\,min} = \frac{2(1-g)}{\cos\,(\alpha_0/2)\,\sqrt{(1+g)^2(\pi-\alpha_0)^2 + 4(1-g)^2 A^2}}$$

$$\varepsilon_{i\,max} = \frac{2\,\sqrt{4\left[2(1+g^2) - (1-g)^2 A\right]^2 + (\pi-\alpha_0)^2(1-g^2)^2}}{\cos\,(\alpha_0/2)\,\sqrt{(1+g)^2(\pi-\alpha_0)^2 + 4(1-g)^2 A^2 - 8(1+g^2)\,A}}\,, \quad (2)$$

where $A = 1 - (\pi-\alpha)\,(tg^2\,\alpha_0)/2$ ; $g = u_{ck}[\Psi_0 + \alpha_0/2] / u_{ck}[\Psi_0 - \alpha_0/2]$ - parameter of the losses in circuit $C_k$ - $W_e$, see fig.2.

Typical form of stable zone of FEM in the area b - $\varepsilon_u$ is presented on fig.3.

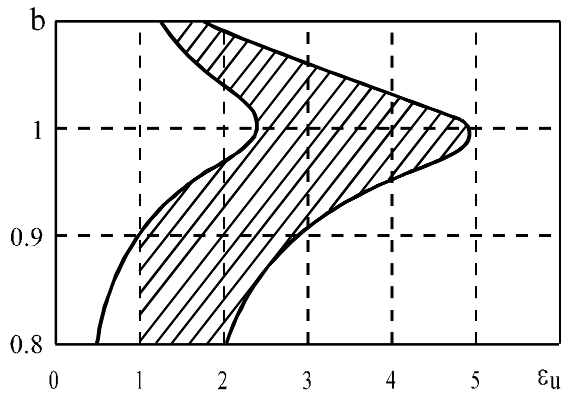


Fig.3. The stable zone of FEM.

The curves on fig.3 and the line $\varepsilon_u = 1$ limit the region of stable ferroresonance oscillations and when the position of operation point is inside it the oscillations are stable when even electrical parameters or temperature are varying.

The corresponding excitation circuit components parameters can be calculated from the equations (for small hysteresis losses and values of $\alpha_0$, see fig. 2):

$$\lambda = \frac{u\,[\Psi_0 - \alpha_0 / \ 2]}{U_{m\,cr}} \cong \frac{\pi(1+g) \pm \{\varepsilon_i^2[4(1-g)^2 + \pi^2(1+g)^2] - 4(1-g)^2\}^{1/2}}{(1-g)^2 + \pi^2(1+g)^2 / 4} \ ;$$

(3)

$$\Psi_0 \cong \arcsin \frac{\pi(1-g)^2 \pm (1-g)\{\varepsilon_i^2[4(1-g)^2 + \pi^2(1+g)^2] - 4(1-g)^2\}^{1/2}}{\varepsilon_i[2(1-g)^2 + \pi^2(1+g)^2/2]} \ ;$$

where $\lambda$ – the ratio between $C_k$ voltage in the beginning of discharge and $U_{mcr}$.

To calculate further the excitation current pulse amplitude (and magnetic field intensity) and other parameters of FEM makes no serious difficulties because they are already linear circuit parameters. At any rate, it is obvious from the foregoing that the calculation of FEM excitation circuit is fairly complicated and is valid only for relatively narrow set of parameters. But for the practical use important is only to have clear understanding of qualitative relation of FEM parameters and of the process in the circuit. In order to provide FEM practically it is enough to proceed as follows.

After the FS core with corresponding number of turns is chosen and excitation frequency is postulated, one can use the equations for linear oscillating circuit, specifying $\alpha_0 \approx 0.1 \div 0.2$, and calculate $C_k$ value. Then $L_g C_g C_k$ circuit has to be tuned slightly below excitation frequency ($b \approx 0.95$, see fig.3) and the stability region of FEM has to be checked. If it is necessary to raise the amplitude of current pulse, $C_k$ has to be magnified and the circuit recalculated etc.

In fact the FEM realization needs higher qualification of circuit designer as other modes, what is, may be, its greatest disadvantage. But the gains are still greater and can not be achieved by any other known means.

As to the phase instability influence, it was eliminated by a special circuit diagram (fig. 4), which synchronizes the commutation pulse of the phase detector (PD) with the moments of the FS core saturation. The diagram of the excitation channel ECH shows that there is a feed-back from excitation circuit (EC) via synchronization pulses former (SPF), which can shift the edge of commutation pulse in dependence from current pulse Im position.

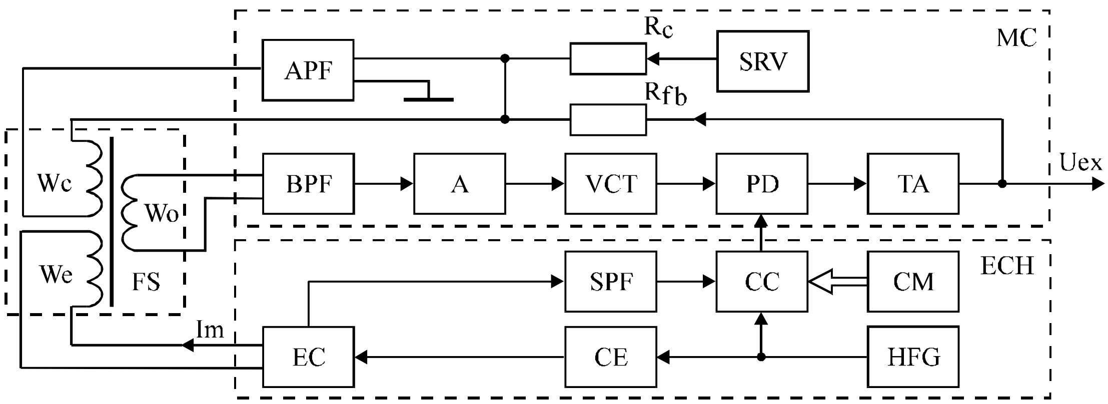


Fig.4. Full functional diagram of FGM.

One of the most difficult problems when precise magnetometer for observatory is constructed is very wide dynamic range of input signals: it is necessary to measure the field about 50000 nT with the sensitivity threshold no more than 0,1 nT. In order to provide such wide dynamics a field compensation in the FS volume is necessary. It seems more convenient to make such compensation with the help of the compensation winding $W_c$ , driving in it the currents from two sources: from the stable source of reference voltage (SRV) via compensation resistor $R_c$ , having a determined number of voltage steps, and from the output of the terminal amplifier (TA) of the measuring channel (MC). Modern SRV have very high stability and the possibility of the development of step controlled SRV with the drift as low as tenth ppm do exists. Between the SRV steps feed-back from TA output compensates the residue and $R_{fb}$ controls the degree of compensation.

The complication is introduced by the fact that the own resistance of the copper wire, forming $W_c$ , is connected seriesly with high precision resistors $R_c$ and $R_{fb}$ , what gives well-known temperature dependence, which is typical for copper. The most effective mode of the compensation of this error seems to be the coupling of the amplifier with parallel feedback (APF) between compensation current sources and $W_c$, in which feed-back loop is $W_c$ itself. Then, if the input current of APF is enough small ( $< 0,1$ nA), the current via $W_c$ will depend only from the sum of currents via $R_c$ and $R_{fb}$ . To have such a current summing point is very convenient for the practical realization of the magnetometer circuit.

Another peculiarity of the magnetometer is the PD design. As it was mentioned, MC must have very wide dynamics (about 120 dB), what typically needs to raise the output power of the second harmonic signal amplifier (A), to the output of which PD is coupled. A new version of this circuit is developed, which has a voltage-current transformer (VCT) between A and PD. In an equilibrium mode a VCT output current is very small but in the transition mode it can achieve high values, providing necessary dynamics. Such a circuit allows to lower the requirements to a band-pass filter (BPF) connected to output winding $W_0$ and so to raise the stability and rapidity of the magnetometer.

All another peculiarities of developed magnetometers belong to their construction. For three-components magnetometer the FS design is similar to the Danish version (O.Rasmussen) with slight differences and includes the marble cube basement with three race-track flux-gate sensors inside quartz tubes for $W_c$ , placed orthogonally, and all this suspended in the thread Cardan for a tilt compensation.

An idea to lower considerably the FS price without decreasing its metrological parameters was worked out. One of such realizations is based on the use of nonmagnetic metallic alloys with big enough but exactly known linear temperature extension factor for manufactoring of FS housing. The appearing by this total temperature drift of FGM was compensated by known in principle but modernized technical means. Such all-metal housing construction especially suits for hard application conditions: space, boreholes etc. It is necessary to mention, that high conductivity of metallic housing creates a turn with low resistance around the sensor and is shunting its output winding. This leads to the sensitivity drop, the elimination of which needs the determination of special requirements to construction parameters which is possible, but rather complicated from both metrological and practical aspects. The influence of short-circuited housing was studied and special operation mode was proposed, what eliminates conductivity influence in principle. Shortly, it is based on two pairs of sensors for each component, operating in such a way that the excitation current pulses for each sensor of the pair were shifted by 90°. By this, when one sensor is in saturation, the second one - not, and vice-versa. It leads to the situation when overall DC magnetic flux via external housing is constant and because of this not damped and only ”switched” from one to other sensor inside.

As to the AC interferences, caused by external magnetic fields, they dissipate very quickly because of high Fuco currents induced by them in the conductive housing.

Besides two- and one-components magnetometers are developed for different geophysical and industrial applications, the measurement range of which is from 0,1 till 500000 nT according to a version. These both have two modifications: with broad frequency band, what allows to use them also for a.c. magnetic field measurement till 1 kHz, and d.c. only with very deep a.c. fields compensation achieved due to the described FS design. The last modification is convenient for magnetic field measurements in industrial conditions: mains frequency and pulse noise do not affect its readings.

The technical parameters of the developed magnetometers are presented in table 2.

Table 2. Main parameters of developed magnetometers.

| Parameter \ Magnetometer version | 1 | 2 | 3 | 4 |
|---|---|---|---|---|
| Compensation range, nT | ± 70 000 | ± 100 000 | - | - |
| Measurement band, nT | ± 2000 | ± 5000 | ± 500 000 | ± 50 000 |
| Resolution, nT | 0.1 | 0.1 | 0.5 | 1 |
| Dynamic range, dB | - | 120 | 70 | 70 |
| Thermal drift, nT/ °C | < 0.1 | < 0.3 | - | - |
| Inorthogonality, min. arc. | < 15 | < 30 | - | - |
| Power consumption, W | < 3.5 | < 2.5 | < 1 | 0.025 |
| Weight, kg | - | < 3 | < 1.5 | 0.1 |
| Output | RS-232 | RS-232 and analog | analog | analog |

Version type:
1) Reference 3-components FGM for observatories. Temporal drift <3 nT/year; tilt compensated.
2) Field / marine 3-components FGM for geophysical survey. 4 1/2 LCD indication.
3) Two / one components portable FGM.
4) Two / one components miniature FGM.

In the conclusion the authors would like to mention that this report summarizes the precedent works, partly published in FSU scientific magazines and patents. But because of practically absent knowledge of western colleagues with these papers the authors decided do not refer them here.

Contact point: Valery Korepanov, Lviv Centre of Institute for Space Research, Naukova str. 5A, 79060 Lviv, Ukraine, Phone/ Fax + 380 322 639163, E-mail: vakor@isr.lviv.ua